

# A full controller for a fixed-wing UAV

Gerardo Flores, Alejandro Flores and Andrés Montes de Oca

**Abstract**—This paper presents a nonlinear control law for the stabilization of a fixed-wing UAV. Such controller solves the path-following problem and the longitudinal control problem in a single control. Furthermore, the control design is performed considering aerodynamics and state information available in the commercial autopilots with the aim of an ease implementation. It is achieved that the closed-loop system is G.A.S. and robust to external disturbances. The difference among the available controllers in the literature is: 1) it depends on available states, hence it is not required extra sensors or observers; and 2) it is possible to achieve any desired airplane state with an ease of implementation, since its design is performed keeping in mind the capability of implementation in any commercial autopilot.

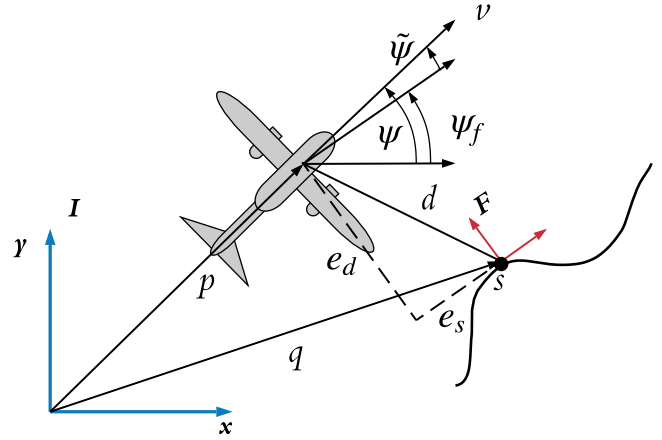
**Index Terms**—Fixed-wing; path-following; UAV; longitudinal aircraft; dynamics Lyapunov-based control.

## I. INTRODUCTION

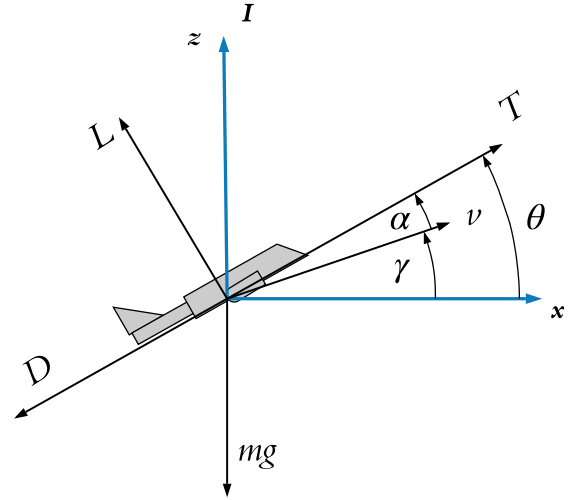
Fixed-wing Unmanned Aerial Vehicles (UAVs) have become relevant above the quadrotors in remote sensing applications, precision agriculture, and surveillance. This is due to its flight endurance, long flying times, high speeds and energy efficiency. Due to the inherent non-linearity condition of fixed-wing UAVs, effective control need to be applied to this type of vehicles so this is a topic that remains being a challenge. In this paper we propose a full controller that achieves to stabilize the airplane in a condition required to perform inspection and surveillance missions. Full control means that it can stabilize the UAV at any desired position and velocity taking into account the optimal angle of attack and aerodynamics. This controller is developed taking in mind its applicability in autopilots such as the popular Pixhawk.

### A. Literature review

In the vast majority of the works relating fixed-wing aircraft control, the problem is tackled based in three fundamental modeling-based cases: a) the longitudinal model where the airspeed, angle of attack and pitch dynamics are controlled; b) path-following in 2D and 3D, where desired  $(x, y)$  and  $(x, y, z)$  positions must be achieved respectively; and c) considering the full 6-DOF airplane mathematical model. Each of these approaches have its own pros and cons. Studying longitudinal model and path-following problem separately, inherits the problem of not considering the full control of the plane. Whereas in the path-following control



(a) Lateral view.



(b) Longitudinal view.

Fig. 1: Diagram of the fixed-wing control problem.

the airspeed and aerodynamics are not considered, in the longitudinal approach the steering of the path is not taken into account. On the other hand, investigating the 6-DOF model-based control usually results in complex controls that includes a great quantity of parameters and terms that makes the implementation in real UAVs a complex task. Some of the most recent works of these three cases are shown at Table I.

Apart from the aforementioned approaches to control fixed-wing UAVs, there is the guidance law that resolves the problem of path following by a simple lateral acceleration

G. Flores, A. Flores and A. Montes de Oca are with the Perception and Robotics Laboratory, Centro de Investigaciones en Óptica, León, Guanajuato, Mexico, 37150. (email: gfflores@cio.mx, alejandrof@cio.mx and andresmr@cio.mx). Corresponding author: Gerardo Flores.

This work was supported partially by the FORDECYT-CONACYT under grant 292399 and by the Laboratorio Nacional de Óptica de la Visión of the CONACYT agreement 293411.

TABLE I: State of the art of fixed-wing UAV controllers.

	6-DOF	Path-following 2D	Path-following 3D	Longitudinal airplane dynamics control
No disturbance	[1]	[2], [3], [4]	[5], [6], [7], [8], [9]	[10], [11], [12], [13]
Disturbance		[14], [15]	[16], [17], [18]	

command; this approach can be seen for instance in [19], and in the famous paper [20] which presents the guidance law implemented in the Pixhawk commercial autopilot.

Regarding control techniques used for solving the control problem there are for instance: backstepping [21], [22], [23]; gain scheduled [24]; sliding mode [25]; model referenced adaptive control [26]; model predictive control [27], [28]; active disturbance rejection control [29]; among others.

### B. Contribution

The motivation to develop this work is twofold: a) present an algorithm that fully controls the fixed-wing UAV considering aerodynamics and the path steering problem; and b) design a controller as simple as possible that effectively stabilizes the system in the complete flight dynamics, i.e. stabilizing aircraft  $(x, y)$  position, angle of attack, pitch dynamics, flight-path angle, yaw dynamics and airspeed (and as a consequence  $z$  dynamics) to some given desired states. The controlled is designed having in mind its implementation in the Pixhawk autopilot using the sensor information available on it.

### C. Paper structure

The rest of the paper is structured as follows. In Section II the fixed-wing mathematical model is described, then based on desired states an error model is obtained. Section III presents the full control that stabilized the complete system, a formal proof is given. Section IV contains the simulation results that validates the effectiveness of the control. Finally, in Section V some comments and future work are presented.

## II. PROBLEM FORMULATION

### A. System Model

Consider the following mathematical model representing the longitudinal and lateral dynamics according to Fig. 1.

$$\begin{aligned} m\dot{v} &= T \cos \alpha - D - mg \sin \gamma \\ mv\dot{\gamma} &= T \sin \alpha + L - mg \cos \gamma \\ m\dot{\theta} &= q \\ I_y \dot{q} &= \tau \end{aligned} \quad (1)$$

$$\begin{aligned} \dot{x} &= v \cos \psi \\ \dot{y} &= v \sin \psi \\ \dot{\psi} &= \omega \end{aligned} \quad (2)$$

where  $v$  is the airspeed of the drone,  $\alpha$ ,  $\gamma$  and  $\theta$  are the angle of attack (AoA), the bank and the pitch angle, respectively,  $D$  and  $L$  are the drag and lift forces generated by the aerodynamics of the wing,  $\dot{x}$  and  $\dot{y}$  are the velocities in the inertial frame  $(I)$ , and  $\psi$  is the yaw angle. As control inputs, the dynamics can be controlled by  $T$ ,  $\tau$  and  $\omega$ . Without loss

of generality, let normalize system (1), i.e.  $m = I_y = 1$  and then it is rewritten as

$$\begin{aligned} \dot{v} &= T \cos \alpha - D - \sin \gamma \\ v\dot{\gamma} &= T \sin \alpha + L - \cos \gamma \\ \dot{\theta} &= q \\ \dot{q} &= \tau. \end{aligned} \quad (3)$$

We need to introduce the error of the angles. So, first, we define the velocity, bank angle and pitch errors as

$$\begin{aligned} \tilde{v} &= v - v_d \\ \tilde{\gamma} &= \gamma - \gamma_d \\ \tilde{\theta} &= \theta - \theta_d. \end{aligned} \quad (4)$$

Using (4) in (3) and considering that  $\tilde{q} = q - q_d$ , then we have

$$\begin{aligned} \dot{\tilde{v}} &= T \cos \alpha - D - \sin(\tilde{\gamma} + \gamma_d) \\ \dot{\tilde{\gamma}} &= \frac{T \sin \alpha + L - \cos(\tilde{\gamma} + \gamma_d)}{\tilde{v} + v_d} \\ \dot{\tilde{\theta}} &= q - q_d \\ \dot{\tilde{q}} &= \tau - \dot{q}_d. \end{aligned}$$

If we define the following coordinate change

$$\tilde{\theta} = \begin{pmatrix} \tilde{\theta}_1 \\ \tilde{\theta}_2 \end{pmatrix} = \begin{pmatrix} \theta - \theta_d \\ q - q_d \end{pmatrix}$$

and consider that  $\tilde{\alpha} = \alpha - \alpha_d$ . The system changes to

$$\begin{aligned} \dot{\tilde{v}} &= T \cos(\tilde{\alpha} + \alpha_d) - D - \sin(\tilde{\gamma} + \gamma_d) \\ \dot{\tilde{\gamma}} &= \frac{T \sin(\tilde{\alpha} + \alpha_d) + L - \cos(\tilde{\gamma} + \gamma_d)}{\tilde{v} + v_d} \\ \dot{\tilde{\theta}}_1 &= \tilde{\theta}_2 \\ \dot{\tilde{\theta}}_2 &= \tau - \dot{q}_d \end{aligned} \quad (5)$$

where  $\dot{\tilde{\theta}}_2 = \tilde{\tau}$ .

For the lateral model, we define orientation and position errors according to Fig. 1a. This path following approach has been investigated in our previous work [4] where a virtual particle that moves over the desired path according to the velocity and heading of the UAV is used to achieve the following task. So, the errors are defined as follows [4]

$$\begin{aligned} \dot{e}_s &= v \cos(\tilde{\psi}) - \dot{s} + Cc(s)e_d \dot{s} \\ \dot{e}_d &= v \sin(\tilde{\psi}) - Cc(s)e_s \dot{s} \\ \dot{\tilde{\psi}} &= \omega - Cc(s)\dot{s} \end{aligned}$$

where  $e_s$  and  $e_d$  are the  $x$  and the  $y$  errors, respectively, between the virtual particle and the position of the UAV in the inertial frame  $(I)$  that is expressed in the velocity particle frame  $(F)$ . This rotation angle is the defined as

$$\psi_f = \arctan \frac{y'_s}{x'_s}$$

It is also introduced the path curvature of the desired trajectory as  $C_c$ . As  $v = \tilde{v} + v_d$ , the previous system now

is

$$\begin{aligned}\dot{e}_s &= (\tilde{v} + v_d) \cos(\tilde{\psi}) - \dot{s} + Cc(s)e_d \dot{s} \\ \dot{e}_d &= (\tilde{v} + v_d) \sin(\tilde{\psi}) - Cc(s)e_s \dot{s} \\ \dot{\tilde{\psi}} &= \omega - Cc(s)\dot{s}\end{aligned}\quad (6)$$

Gathering (5) and (6), the complete error model is given by

$$\begin{aligned}\dot{\tilde{v}} &= T \cos(\tilde{\alpha} + \alpha_d) - D - \sin(\tilde{\gamma} + \gamma_d) \\ \dot{\tilde{\gamma}} &= \frac{T \sin(\tilde{\alpha} + \alpha_d) + L - \cos(\tilde{\gamma} + \gamma_d)}{\tilde{v} + v_d} \\ \dot{\tilde{\theta}}_1 &= \tilde{\theta}_2 \\ \dot{\tilde{\theta}}_2 &= \tilde{\tau} \\ \dot{e}_s &= v \cos(\tilde{\psi}) - \dot{s} + Cc(s)e_d \dot{s} \\ \dot{e}_d &= v \sin(\tilde{\psi}) - Cc(s)e_s \dot{s} \\ \dot{\tilde{\psi}} &= \omega - Cc(s)\dot{s}.\end{aligned}\quad (7)$$

### III. MAIN RESULT

In this section the main result is resented. For that, let consider the following assumptions.

*Assumption 1:* The airspeed velocity is always positive, i.e.  $v \in (0, c]$  with  $c \in \mathbb{R}^+$ .

*Assumption 2:*  $v_d$  and  $\gamma_d$  are considered constants.

*Assumption 3:* The initial airspeed is positive, i.e., the fixed-wing UAV has taken off and is flying in the air.

The main results is presented in the next

*Theorem 1:* Let system (7) under controls (14), (16), (22) and (24) then the closed loop system is globally asymptotically stable.

*Proof:* The goal is to get  $v \rightarrow v_d$  and  $\alpha \rightarrow \alpha_d$  with  $v_d, \alpha_d \in \mathbb{R}^+$ . It is important to highlight that the algebraic equation  $\theta = \gamma + \alpha$  must be always fulfilled. This is a condition inherent of the AoA, pitch and flight-path angle. Let consider the following  $C^1$  function

$$\tilde{V}_1 = \tilde{V}_{\tilde{v}} + \tilde{V}_{\tilde{\gamma}} + \tilde{V}_{\tilde{\theta}} \quad (8)$$

where

$$\tilde{V}_{\tilde{v}} = \frac{1}{2}\tilde{v}^2; \quad \tilde{V}_{\tilde{\gamma}} = \frac{1}{2}\tilde{\gamma}^2; \quad \tilde{V}_{\tilde{\theta}} = \tilde{\theta}^T P \tilde{\theta} \quad (9)$$

with  $P = P^T > 0$ . The time derivative of  $\tilde{V}_{\tilde{v}}$  is

$$\dot{\tilde{V}}_{\tilde{v}} = \tilde{v}\dot{\tilde{v}} = \tilde{v}(T \cos(\tilde{\alpha} + \alpha_d) - D - \sin(\tilde{\gamma} + \gamma_d))$$

where we have designed the control term  $T \cos(\tilde{\alpha} + \alpha_d)$  as

$$T \cos(\tilde{\alpha} + \alpha_d) = D + \sin(\tilde{\gamma} + \gamma_d) - k_v \tilde{v} \quad (10)$$

and then under this control the time derivative of  $\tilde{V}_{\tilde{v}}$  results in

$$\dot{\tilde{V}}_{\tilde{v}} = -k_v \tilde{v}^2. \quad (11)$$

Now obtaining the time derivative of  $\tilde{V}_{\tilde{\gamma}}$  we obtain

$$\dot{\tilde{V}}_{\tilde{\gamma}} = \tilde{\gamma}(T \sin(\tilde{\alpha} + \alpha_d) + L - \cos(\tilde{\gamma} + \gamma_d)) \frac{1}{\tilde{v} + v_d}$$

where we choose the control term  $T \sin(\tilde{\alpha} + \alpha_d)$  equal to

$$T \sin(\tilde{\alpha} + \alpha_d) = -L + \cos(\tilde{\gamma} + \gamma_d) - (\tilde{v} + v_d)(k_\gamma \tilde{\gamma}) \quad (12)$$

and therefore

$$\dot{\tilde{V}}_{\tilde{\gamma}} = -k_\gamma \tilde{\gamma}^2. \quad (13)$$

Considering  $u_1 = T \cos(\tilde{\alpha} + \alpha_d)$  and  $u_2 = T \sin(\tilde{\alpha} + \alpha_d)$  as temporal control inputs, we can extract  $T$  as

$$T = \sqrt{u_1^2 + u_2^2} \quad (14)$$

$\alpha_d$  is obtained from  $u_2 = T \sin \alpha$  obtaining  $\alpha$  as follows

$$\alpha_d = \arcsin\left(\frac{u_2}{T}\right), \quad (15)$$

this  $\alpha_d$  is the commanded for  $\theta_d = \alpha_d + \gamma_d$ . The pitch error subsystem can be represented by

$$\dot{\tilde{\theta}} = A \tilde{\theta} + B \tilde{\tau} \quad \text{with} \quad A = \begin{pmatrix} 0 & 1 \\ 0 & 0 \end{pmatrix}; \quad B = \begin{pmatrix} 0 \\ 1 \end{pmatrix}.$$

Let

$$\tilde{\tau} = -k_{\tilde{\theta}_1} \tilde{\theta}_1 - k_{\tilde{\theta}_2} \tilde{\theta}_2 \quad (16)$$

then  $\dot{\tilde{\theta}} = \tilde{A} \tilde{\theta}$  where  $\tilde{A} = \begin{pmatrix} 0 & 1 \\ -k_1 & -k_2 \end{pmatrix}$ . It follows that

$$\dot{\tilde{V}}_{\tilde{\theta}} = \tilde{\theta}^T (P \tilde{A} + \tilde{A}^T P) \tilde{\theta} = -\tilde{\theta}^T Q \tilde{\theta} \quad (17)$$

with the Lyapunov equation  $P \tilde{A} + \tilde{A}^T P = -Q$  with  $Q = Q^T > 0$ . Then, it follows that the time derivative of (8) is given by

$$\dot{\tilde{V}}_1 = -k_v \tilde{v}^2 - k_\gamma \tilde{\gamma}^2 - \tilde{\theta}^T Q \tilde{\theta} \leq 0 \quad (18)$$

From the previous analysis one concludes that all trajectories  $E(t) = (\tilde{v}(t), \tilde{\gamma}(t), \tilde{\theta}_1(t), \tilde{\theta}_2(t), \tilde{e}_s(t), \tilde{e}_d(t), \tilde{\psi}(t))$  are bounded, i.e. for each trajectory  $E(t)$  there is an  $R \in \mathbb{R}$  such that  $\|E(t)\| \leq R \forall t \geq 0$ .

It is known that any bounded trajectory of an autonomous system like (7), converges to an invariant set [30]. Let such system invariant set be  $\Omega_l$ . By construction we can say that

$$\Omega_l = \{E(t) \in \mathbb{R}^7 : \tilde{V}(E) \leq l\} \quad (19)$$

where  $\tilde{V}(E)$  is a Lyapunov function for (7). Let find  $\tilde{V}(E)$  by combining  $\tilde{V}_1$ , which is not dependent of every states in (7), with the positive definite function

$$\tilde{V}_2 = \tilde{V}_{\tilde{e}_s} + \tilde{V}_{\tilde{e}_d} + \tilde{V}_{\tilde{\psi}} \quad (20)$$

where

$$\tilde{V}_{\tilde{e}_s} = \frac{1}{2}e_s^2; \quad \tilde{V}_{\tilde{e}_d} = \frac{1}{2}e_d^2; \quad \tilde{V}_{\tilde{\psi}} = \frac{1}{2}(\tilde{\psi} - \delta(e_d))^2 \quad (21)$$

where  $\delta(e_d)$  is a function which is saturated as in [31] that satisfies the condition  $e_d \delta(e_d) \leq 0 \forall e_d$ . Let's compute the time derivative of  $\tilde{V}_{\tilde{e}_s} + \tilde{V}_{\tilde{e}_d}$  and then we get

$$\begin{aligned}\dot{\tilde{V}}_{\tilde{e}_s} + \dot{\tilde{V}}_{\tilde{e}_d} &= e_s \dot{e}_s + e_d \dot{e}_d = e_s [(\tilde{v} + v_d) \cos \tilde{\psi} - \dot{s} + Cc(s)e_d \dot{s}] \\ &\quad + e_d [(\tilde{v} + v_d) \sin \tilde{\psi} - Cc(s)e_s \dot{s}].\end{aligned}$$

If we define  $\dot{s}$  as

$$\dot{s} = k_s \text{sign}(e_s) + (\tilde{v} + v_d) \cos \tilde{\psi} \quad (22)$$

then

$$\dot{\tilde{V}}_{\tilde{e}_s} + \dot{\tilde{V}}_{\tilde{e}_d} = -k_s |e_s| + (\tilde{v} + v_d) e_d \sin \tilde{\psi}. \quad (23)$$

Now if we obtain the time derivative of  $\tilde{V}_{\tilde{\psi}}$

$$\begin{aligned} \dot{\tilde{V}}_{\tilde{\psi}} &= (\tilde{\psi} - \delta(e_d))(\omega - Cc(s)\dot{s}) \\ &\quad - \dot{\delta}[(\tilde{v} + v_d) \sin \tilde{\psi} - Cc(s)e_s \dot{s}] \end{aligned}$$

then consider the following proposed control

$$\begin{aligned} \omega &= Cc(s)\dot{s} + \dot{\delta}[(\tilde{v} + v_d) \sin \tilde{\psi} - Cc(s)e_s \dot{s}] \\ &\quad - (\tilde{v} + v_d)e_d \left( \frac{\sin \tilde{\psi} - \sin \delta}{\tilde{\psi} - \delta} \right) - k_{\omega} \text{sign}(\tilde{\psi} - \delta) \end{aligned} \quad (24)$$

then

$$\dot{\tilde{V}}_{\tilde{\psi}} = -(\tilde{v} + v_d)e_d \sin \tilde{\psi} + (\tilde{v} + v_d)e_d \sin \delta - k_{\omega} |\tilde{\psi} - \delta(e_d)|. \quad (25)$$

Using (23) and (25) in (20), it follows that

$$\begin{aligned} \dot{\tilde{V}}_2 &= -k_s |e_s| + \tilde{v}e_d \sin \delta(e_d) + v_d e_d \sin \delta(e_d) \\ &\quad - k_{\omega} |\tilde{\psi} - \delta(e_d)|. \end{aligned} \quad (26)$$

Then, as

$$\dot{\tilde{V}} = \dot{\tilde{V}}_1 + \dot{\tilde{V}}_2$$

we substitute (18) and (26)

$$\begin{aligned} \dot{\tilde{V}} &= -k_v \tilde{v}^2 - k_{\gamma} \tilde{\gamma}^2 - \tilde{\theta}^T Q \tilde{\theta} - k_s |e_s| + \tilde{v}e_d \sin \delta(e_d) \\ &\quad + v_d e_d \sin \delta(e_d) - k_{\omega} |\tilde{\psi} - \delta(e_d)| \end{aligned} \quad (27)$$

From (19) it follows that

$$|\tilde{V}| = \sqrt{2l}. \quad (28)$$

Then if we define  $a$  from (27) as

$$a = -k_v \tilde{v}^2 - k_{\gamma} \tilde{\gamma}^2 - \tilde{\theta}^T Q \tilde{\theta} - k_s |e_s| - k_{\omega} |\tilde{\psi} - \delta(e_d)| \quad (29)$$

and we substitute (29) and (28) in (27) we have

$$\dot{\tilde{V}} \leq a + \sqrt{2l} |e_d \sin \delta(e_d)| + v_d e_d \sin \delta(e_d)$$

and

$$\begin{aligned} a + \sqrt{2l} |e_d \sin \delta(e_d)| + v_d e_d \sin \delta(e_d) \\ \leq a - (v_d - \sqrt{2l}) |e_d \sin \delta(e_d)| \end{aligned}$$

since  $-|e_d \sin \delta(e_d)| = e_d \sin \delta(e_d)$ , then  $\dot{\tilde{V}} \leq 0$  if  $v_d > \sqrt{2l}$ . Also, if  $\tilde{\psi} = \delta(e_d)$  and the remaining states are zero,  $\dot{\tilde{V}} = 0$ . Then it is clear that  $\tilde{V} > 0 \forall E(t) \neq 0$  and  $\dot{\tilde{V}}(E(t)) \leq 0 \forall E(t)$  in  $\Omega_l$ . Let  $S \subseteq \Omega_l$  the set of all points where  $\dot{\tilde{V}} = 0$  given by

$$\dot{\tilde{V}} = 0 = -k_{\omega} |\tilde{\psi} - \delta(e_d)| \rightarrow \tilde{\psi} = \delta(e_d).$$

Note that the rest of  $\dot{\tilde{V}}$  is equal to zero at zero. Observing the closed loop system (7) with the controls (14), (16) and (24) when  $\tilde{v} = \tilde{\gamma} = \tilde{\theta}_1 = \tilde{\theta}_2 = e_s = 0$  and  $\tilde{\psi} = \delta(e_d)$  one obtains

$$\begin{aligned} \dot{e}_s &= 0 = v_d \cos \tilde{\psi} - v_d \cos \tilde{\psi} + Cc(s)e_d [v_d \cos \tilde{\psi}] \\ &= Cc(s)v_d e_d \cos \delta(e_d) \\ \dot{e}_d &= 0 = v_d \sin \tilde{\psi} \\ \dot{\tilde{\psi}} &= \dot{\delta}(v_d \sin \tilde{\psi}) \end{aligned} \quad (30)$$

then  $e_d = \tilde{\psi} = 0$  is the only solution of (30) and therefore the largest invariant set  $M$  in  $S$  is the origin  $E(t) = 0$  and by the LaSalle invariance principle  $E(t) \rightarrow 0$  as  $t \rightarrow \infty$ ; as

long as the initial state  $E_0(t)$  be in  $\Omega_e$ . And the closed loop system is asymptotically stable in the arbitrary large set:  $\Omega_e$  provided that  $\sqrt{2l} \leq v_d$ . Also  $\tilde{V} \rightarrow \infty$  as  $|E(t)| \rightarrow \infty$ , i.e.  $\tilde{V}$  is radially unbounded, then the closed loop system is G.A.S.  $\blacksquare$

#### IV. SIMULATION EXPERIMENTS

To verify the stability in a computational environment, a numerical simulation of the systems (1) and (2) under controls (14), (16), (22) and (24) is performed. The parameters used in the simulation are:  $\psi_a = \frac{\pi}{2.1}$ ,  $m = 3$ ,  $g = 9.81$ ,  $I_y = 1$ ,  $k_{\tilde{\theta}_1} = 10$ ,  $k_{\tilde{\theta}_2} = 5$ ,  $k_v = 50$ ,  $k_s = 2$ ,  $k_{\gamma} = 2$ ,  $k_{\omega} = 20.25$ ,  $\gamma_d = 1^\circ$ ,  $V_d = \sqrt{\frac{m \cdot g}{.96 * c}}$ , where  $c = \frac{\rho S}{2}$  is a constant that describes the air density an the area of the wind. The initial conditions for the simulation are:  $s_0 = 0$ ,  $x_0 = 10$ ,  $y_0 = -5$ ,  $\psi_0 = 0^\circ$ ,  $\gamma_0 = 8^\circ$ ,  $\theta_0 = 8^\circ$ ,  $V_0 = 1$ . The induced disturbance to the  $\psi$  state is a sinusoidal signal with 20 units of amplitude and a frequency of  $0.5 \frac{rad}{s}$ . The airspeed is depicted at Fig. 2. The control  $T$  applied to the model is shown in Fig. 3.

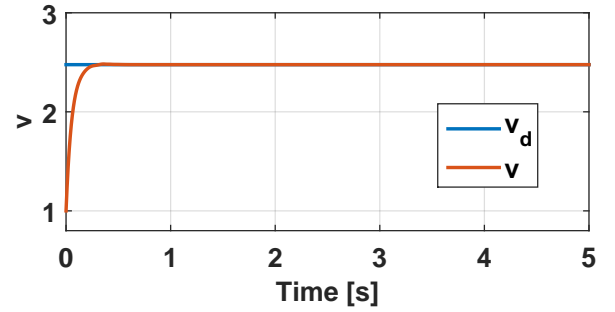


Fig. 2: Airspeed  $v$  through the UAV control for the optimal AoA considering aerodynamics of [32].

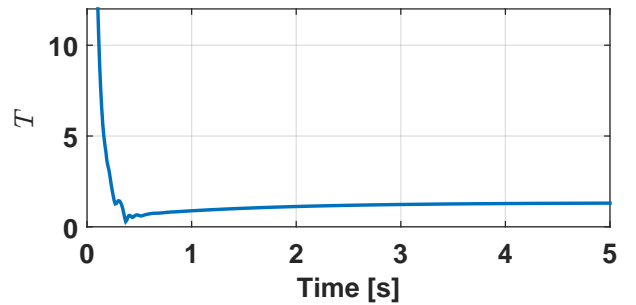


Fig. 3: Thrust control  $T$  applied to the fixed-wing UAV.

Another important fact that determines an optimal flight of the UAV is the AoA. According to the lift coefficient of the wing profile used for this simulation, which is a symmetric profile, the best AoA in relation with the lift-drag coefficients is around  $6^\circ$ . Then, it is expected that this angle is reached during stabilization process. This AoA and

the other aerodynamic terms have been taken from the UAV presented in our previous work [32]. In Fig. 4 it is shown the angles evolution including the AoA convergence to the desired value equal to  $6^\circ$ . The control input  $\tau$  is shown at Fig.

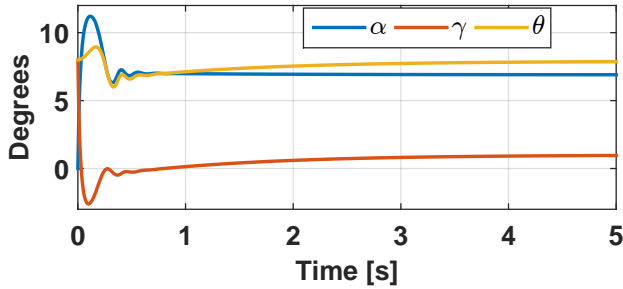


Fig. 4: UAV angles  $\alpha$ ,  $\gamma$  and  $\theta$  keeping the property of  $\theta = \alpha + \gamma$ .

5. With this control it is possible to reach the  $\theta_d$  according to  $\gamma_d$  and  $\alpha_d$ .

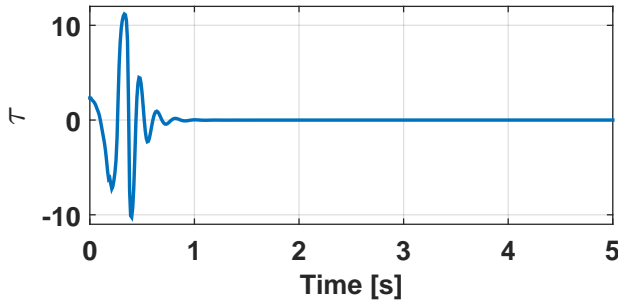


Fig. 5: Control  $\tau$  for the UAV pitch angle.

In Fig.6, the control  $\omega$  is plotted. With this control,  $\psi$  is guided to the desired heading for the path following. Finally, Figs. 7 and 8 depict the UAV's position w.r.t. the desired path, which is in this case a circle of radius 20 with and without disturbance in  $\psi$ , respectively.

## V. CONCLUSIONS

We have presented a full controller for a fixed-wing UAV which presents robust capabilities for disturbances presented in the UAV dynamics. A stability proof is presented which demonstrated that the closed-loop system is GAS.

As future work we intend to implement this controller used the approach known as hardware in the loop (HIL) and finally be implemented in the real fixed-wing UAV in a Pixhawk autopilot.

## REFERENCES

[1] Y. Hamada, T. Tsukamoto, and S. Ishimoto, "Receding horizon guidance of a small unmanned aerial vehicle for planar reference path following," *Aerospace Science and Technology*, vol. 77, pp. 129–137, June 2018.

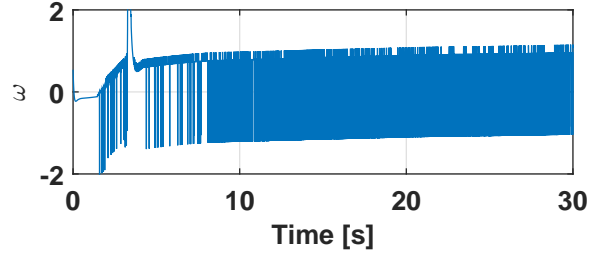


Fig. 6:  $\omega$  control applied to the  $\psi$  state in the system.

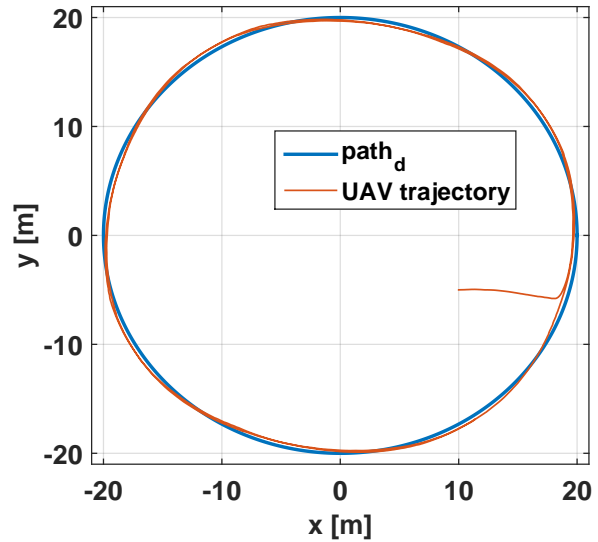


Fig. 7: UAV  $(x, y)$  position during the simulation; and the desired path with disturbance in  $\psi$ .

[2] S. Zhao, X. Wang, Z. Lin, D. Zhang, and L. Shen, "Integrating Vector Field Approach and Input-to-State Stability Curved Path Following for Unmanned Aerial Vehicles," *IEEE Transactions on Systems, Man, and Cybernetics: Systems*, pp. 1–8, 2018.

[3] R. P. Jain, A. P. Aguiar, and J. Sousa, "Self-triggered cooperative path following control of fixed wing Unmanned Aerial Vehicles," in *2017 International Conference on Unmanned Aircraft Systems (ICUAS)*. Miami, FL, USA: IEEE, June 2017, pp. 1231–1240.

[4] G. Flores, I. Lugo-Crdenas, and R. Lozano, "A nonlinear path-following strategy for a fixed-wing mav," in *2013 International Conference on Unmanned Aircraft Systems (ICUAS)*, May 2013, pp. 1014–1021.

[5] I. Kaminer, A. Pascoal, E. Xargay, N. Hovakimyan, C. Cao, and V. Dobrokhodov, "Path Following for Small Unmanned Aerial Vehicles Using L1 Adaptive Augmentation of Commercial Autopilots," *Journal of Guidance, Control, and Dynamics*, vol. 33, no. 2, pp. 550–564, Mar. 2010.

[6] G. Vanegas, F. Samaniego, V. Girbes, L. Armesto, and S. Garcia-Nieto, "Smooth 3d path planning for non-holonomic UAVs," in *2018 7th International Conference on Systems and Control (ICSC)*. Valencia: IEEE, Oct. 2018, pp. 1–6.

[7] T. Oliveira, A. P. Aguiar, and P. Encarnacao, "Three dimensional moving path following for fixed-wing unmanned aerial vehicles," in *2017 IEEE International Conference on Robotics and Automation (ICRA)*. Singapore, Singapore: IEEE, May 2017, pp. 2710–2716.

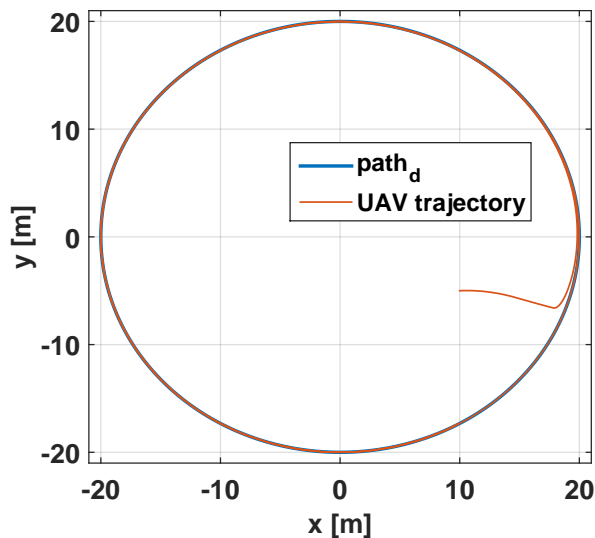


Fig. 8: UAV  $(x,y)$  position during the simulation; and the desired path without disturbance.

- [8] N. Cho, Y. Kim, and S. Park, "Three-Dimensional Nonlinear Differential Geometric Path-Following Guidance Law," *Journal of Guidance, Control, and Dynamics*, vol. 38, no. 12, pp. 2366–2385, Dec. 2015.
- [9] Y. Liang, Y. Jia, J. Du, and J. Zhang, "Vector field guidance for three-dimensional curved path following with fixed-wing UAVs," in *2015 American Control Conference (ACC)*. Chicago, IL, USA: IEEE, July 2015, pp. 1187–1192.
- [10] M. G. Michailidis, K. Kanistras, M. Agha, M. J. Rutherford, and K. P. Valavanis, "Robust nonlinear control of the longitudinal flight dynamics of a circulation control fixed wing UAV," in *2017 IEEE 56th Annual Conference on Decision and Control (CDC)*. Melbourne, Australia: IEEE, Dec. 2017, pp. 3920–3927.
- [11] D. Kong, Q. Geng, Q. Hu, and J. Shao, "Longitudinal control law design for fixed-wing UAV based on multi-model technique," in *Fifth International Conference on Intelligent Control and Information Processing*. Dalian, China: IEEE, Aug. 2014, pp. 48–52.
- [12] J. D. Brigido-Gonzalez and H. Rodriguez-Cortes, "Adaptive energy based control for the longitudinal dynamics of a fixed-wing aircraft," in *2014 American Control Conference*. Portland, OR, USA: IEEE, June 2014, pp. 715–720.
- [13] M. Michailidis, K. Kanistras, M. Agha, M. J. Rutherford, and K. Valavanis, "Nonlinear control of fixed-wing uavs with time-varying aerodynamic uncertainties via  $\mu$ -synthesis," 12 2018, pp. 6314–6321.
- [14] J. Fortuna and T. I. Fossen, "Cascaded line-of-sight path-following and sliding mode controllers for fixed-wing UAVs," in *2015 IEEE Conference on Control Applications (CCA)*. Sydney, Australia: IEEE, Sept. 2015, pp. 798–803.
- [15] Y. Liang, Y. Jia, Z. Wang, and F. Matsuno, "Combined vector field approach for planar curved path following with fixed-wing UAVs," in *2015 American Control Conference (ACC)*. Chicago, IL, USA: IEEE, July 2015, pp. 5980–5985.
- [16] M. C. Palframan, K. T. Guthrie, and M. Farhood, "An LPV path-following controller for small fixed-wing UAS," in *2015 54th IEEE Conference on Decision and Control (CDC)*. Osaka: IEEE, Dec. 2015, pp. 97–102.
- [17] R. W. Beard, J. Ferrin, and J. Humpherys, "Fixed Wing UAV Path Following in Wind With Input Constraints," *IEEE Transactions on Control Systems Technology*, vol. 22, no. 6, pp. 2103–2117, Nov. 2014.
- [18] C. Liu, O. McAree, and W.-H. Chen, "Path-following control for small fixed-wing unmanned aerial vehicles under wind disturbances," *International Journal of Robust and Nonlinear Control*, pp. n/a–n/a, Dec. 2012.
- [19] J. Zhang, Q. Li, N. Cheng, and B. Liang, "Path-following control for fixed-wing unmanned aerial vehicles based on a virtual target," *Proceedings of the Institution of Mechanical Engineers, Part G: Journal of Aerospace Engineering*, vol. 228, no. 1, pp. 66–76, Jan. 2014.
- [20] S. Park, J. Deyst, and J. How, "A New Nonlinear Guidance Logic for Trajectory Tracking," in *AIAA Guidance, Navigation, and Control Conference and Exhibit*. Providence, Rhode Island: American Institute of Aeronautics and Astronautics, Aug. 2004.
- [21] S. Zhao, X. Wang, W. Kong, D. Zhang, and L. Shen, "A novel backstepping control for attitude of fixed-wing uavs with input disturbance," in *2015 34th Chinese Control Conference (CCC)*, July 2015, pp. 693–697.
- [22] A. SaiCharanSagar, S. Vaitheeswaran, and P. Shendge, "Uncertainty estimation based approach to attitude control of fixed wing uav," *IFAC-PapersOnLine*, vol. 49, no. 1, pp. 278 – 283, 2016, 4th IFAC Conference on Advances in Control and Optimization of Dynamical Systems ACODS 2016.
- [23] F. Gavilan, R. Vazquez, and S. Esteban, "Trajectory tracking for fixed-wing uav using model predictive control and adaptive backstepping," *IFAC-PapersOnLine*, vol. 48, no. 9, pp. 132 – 137, 2015, 1st IFAC Workshop on Advanced Control and Navigation for Autonomous Aerospace Vehicles ACNAAV15.
- [24] P. Poksawat, L. Wang, and A. Mohamed, "Gain scheduled attitude control of fixed-wing uav with automatic controller tuning," *IEEE Transactions on Control Systems Technology*, vol. 26, no. 4, pp. 1192–1203, July 2018.
- [25] L. Melkou, M. Hamerlain, and A. Rezug, "Fixed-wing uav attitude and altitude control via adaptive second-order sliding mode," *Arabian Journal for Science and Engineering*, vol. 43, no. 12, pp. 6837–6848, Dec 2018.
- [26] W. Zhou, K. Yin, R. Wang, and Y.-E. Wang, "Design of attitude control system for uav based on feedback linearization and adaptive control," *Mathematical Problems in Engineering*, vol. 2014, pp. 1–8, 03 2014.
- [27] P. Oettershagen, A. Melzer, S. Leutenegger, K. Alexis, and R. Siegwart, "Explicit model predictive control and 11-navigation strategies for fixed-wing uav path tracking," in *22nd Mediterranean Conference on Control and Automation*, June 2014, pp. 1159–1165.
- [28] T. Stastny and R. Siegwart, "Nonlinear model predictive guidance for fixed-wing uavs using identified control augmented dynamics," in *2018 International Conference on Unmanned Aircraft Systems (ICUAS)*, June 2018, pp. 432–442.
- [29] Y. Chen, J. Liang, C. Wang, and Y. Zhang, "Combined of lyapunov-stable and active disturbance rejection control for the path following of a small unmanned aerial vehicle," *International Journal of Advanced Robotic Systems*, vol. 14, no. 2, 2017.
- [30] J. Slotine and W. Li, *Applied Nonlinear Control*. Prentice Hall, 1990.
- [31] I. Fantoni, A. Zavala, and R. Lozano, "Global stabilization of a pvtol aircraft with bounded thrust," in *Proceedings of the 41st IEEE Conference on Decision and Control, 2002.*, vol. 4, Dec 2002, pp. 4462–4467 vol.4.
- [32] A. Flores, A. M. de Oca, and G. Flores, "A simple controller for the transition maneuver of a tail-sitter drone," in *2018 IEEE Conference on Decision and Control (CDC)*, Dec 2018, pp. 4277–4281.